Polymer 49 (2008) 2440–2443

Contents lists available at ScienceDirect

Polymer

journal homepage: www.elsevier.com/locate/polymer

Study of dispersive mobility in polyimide by surface voltage decay measurements

A. Aragoneses*, M. Mudarra, J. Belana, J.A. Diego

Dept. Física i Enginyeria Nuclear, ETSEIAT, C. Colom, 11 Terrassa 08222, Barcelona, Spain

ARTICLE INFO

Article history:
Received 26 September 2007
Received in revised form 4 February 2008
Accepted 26 March 2008
Available online 28 March 2008

PACS:
72.10.Bg
72.20.jv
72.80.Ng
73.50.-h

Keywords:
Conductivity
Polyimide
Dispersive conductivity

ABSTRACT

In order to study charge trapping and transport in polyimide, we have submitted samples of Kapton HN to corona charging and measured its surface potential decay with an electrostatic voltmeter. We propose a two terms mobility to explain the experimental data: a non-dispersive contribution based on Toomer and Lewis model added to a dispersive process, which is associated with the disordered structure of the material. The non-dispersive model alone did not fit well to the data for short times, but our assumption makes the theoretical expression fit successfully to the experimental data. Some important parameters related to the charge transport properties of the material are determined and discussed.

1. Introduction

The use of polyimide (PI) has become widespread in aerospace industry because of its high performances as thermal and electrical insulators. Due to its properties, this material is used as a thermal blanket to prevent artificial satellite systems from wide temperature oscillations. Satellites in space environment are exposed to intense radiations (energetic electrons, ions, X-rays,…) that charge its surface electrically. Polyimide, as it happens in other insulating materials, becomes charged electrically when it is subjected to radiation, so that spontaneous discharges may arise that can lead to malfunctions of the sensitive systems on board [1–4]. In order to improve its mechanical and electrical properties, some studies on PI have been carried out, which propose new synthesis processes [5], fabrication of composites with carbon nanotubes [6] and with silica [7].

There have been registered a few cases where normal operation of board electronics have been interrupted due to spacecraft charging [8]. Understanding and controlling the processes that lead to space charge formation and relaxation in this material are, thus, relevant in order to improve the performance of such blankets. The aim of this paper is to study the space charge relaxation in polyimide, in order to characterize the microscopic processes that contribute to the mobility of the carriers.

Surface potential decay experiments are widely used to study charge transport in polymers [9–15]. In these experiments a film of polymer is submitted to a discharge from a needle and the ions produced are injected on the surface of the film. Electrons or holes move towards the rear electrode due to their own electric field in order to reach electrical equilibrium. Several authors have proposed models to describe these processes [16–20]. Carriers in this situation do not move with the proper mobility of the band, but their mobility is modulated by the presence of traps and by the influence of other carriers. That is why an effective mobility

$$\mu_{\mathrm{eff}}(t) = \mu_0 \eta(t) \tag{1}$$

has to be considered, where μ_0 is the proper mobility in the band and $\eta(t)$ is the ratio of carriers contributing to the process at a time t.

2. Theory

In the case of amorphous materials, discrete trapping levels or bands of trapping levels appear at the bottom of the conduction band (traps for electrons) and the top of the valence band (traps for holes). Carrier mobility is affected by the presence of such trapping levels. Electrons near the bottom of the conduction band move

* Corresponding author.
E-mail address: andres.aragoneses@upc.edu (A. Aragoneses).

0032-3861/$ – see front matter © 2008 Elsevier Ltd. All rights reserved.
doi:10.1016/j.polymer.2008.03.037

between extended states by hopping. Such process requires no thermal activation and leads to relatively high mobilities of about $10\,cm^2\,V^{-1}\,s^{-1}$. If the electron is captured by a trap, its mobility becomes orders of magnitude smaller (analogous process may happen for holes at the top of the valence band). Electron captured by a shallow trap needs thermal energy to perform a thermally activated hopping process, resulting in mobilities of about $10^{-3}\,cm^2\,V^{-1}\,s^{-1}$. Carriers located in deep traps experience very long capture time and their mobility becomes very small ($10^{-10}\,cm^2\,V^{-1}\,s^{-1}$ to $10^{-17}\,cm^2\,V^{-1}\,s^{-1}$). Therefore, a sharp variation of the mobility is expected at levels close to both, the bottom of the conduction band and the top of the valence band, which determines the mobility edges, resulting in a trap modulated mobility [21–23].

The distances between various neighboring trapping sites have some variations about a mean value and even a distribution in trapping energy levels may happen. As transition times which determine the kinetics of the process sensitively depend on these differences in distance and energy, they will suffer a wide statistical dispersion, which results in a mobility that shows a power time dependence in the time domain (dispersive mobility) [24]. This dispersive behavior is reflected by a sublinear frequency dependence in frequency domain measurements of the conductivity [25].

We shall consider that charge transport through the sample is due to two contributions in order to explain the surface potential decay observed in PI. One contribution is associated with a non-dispersive transport process and the other with a dispersive transport process. Charges travelling through the sample may become trapped, so that only a fraction of them contributes to mobility. This lowers the density of carriers of the leading charges' line, so that there are less charges competing for the traps and the effective correlation diminishes, that is why we can expect the dispersive term to be more important for short times. Taking this into account, we can write the effective mobility as

$$\mu_{\mathrm{eff}}(t) = \mu_{\mathrm{N}}(t) + \mu_{\mathrm{D}}(t) = \mu_0(\eta_{\mathrm{N}}(t) + \eta_{\mathrm{D}}(t)) \tag{2}$$

where subindex N refers to the non-dispersive process and D to the dispersive one.

2.1. Non-dispersive mobility

In the case of non-dispersive transport, we consider that charges are injected into the bulk immediately after the corona injection. The band structure can provide several kinds of traps for the charge carriers with different energetic depths. The initial charge spreads into the different traps, a_i being the portion of the initial charge trapped in the state $i = 1 \ldots n$, with $\sum_{i=1}^{n} a_i = 1$. Charges drift through the sample hopping from one localized state to another, r_{ri} being the probability per unit time of a charge to release from a trapping level i and r_{ti} the probability per unit time to be retrapped at trapping level i. In this case the function $\eta(t)$ has the form [26]:

$$\eta_N(t) = LT^{-1}\left[\frac{1}{s}\frac{1}{1+\sum_{i=1}^{n}\frac{r_{\mathrm{ti}}}{s+r_{\mathrm{ri}}}a_i}\right] \tag{3}$$

where LT refers to the Laplace transform of the function and s is the reciprocal time.

In order to ensure our assumption that all charges are injected instantaneously, we have applied a high enough electric field to the needle. In this case charges do not fall into surface traps from where they jump to the bulk, but they are injected directly into the bulk, where the dynamics of charge transport occurs by hopping between localized trapping centers. In our study we consider the simplest case: we assume that the existence of one trapping level thermally connected and that thermally disconnected levels are filled. Therefore, Eq. (3) can be written as

$$\eta_{\mathrm{N}}(t) = LT^{-1}\left[\frac{1}{s}\frac{1}{1+\frac{r_{\mathrm{t}}}{s+r_{\mathrm{r}}}}\right] \tag{4}$$

Transformation of Eq. (4) to time domain leads to

$$\eta_{\mathrm{N}}(t) = \frac{r_{\mathrm{r}} + r_{\mathrm{t}}\ \mathrm{e}^{-Rt}}{R} \quad (R = r_{\mathrm{r}} + r_{\mathrm{t}}) \tag{5}$$

This expression was previously found by Toomer and Lewis, who considered the dynamics of the hopping transport, and defined [18]

$$\mu_{\mathrm{eff}}(n_{\mathrm{f}} + n_{\mathrm{t}}) = \mu_0 n_{\mathrm{f}} \tag{6}$$

where n_{t} refers to trapped charge and n_{f} refers to free charge, the one that contributes to mobility.

When charges get the grounded rear electrode they do not contribute any more to the surface potential that we measure, so the decay behaves differently during the travel of the leading charges than after they have reached the grounded electrode. The time this front of charges takes to get through the sample is the transit time, t_τ. We shall limit our study to $t < t_\tau$. Up to the transit time the derivative of the surface potential can be written [18] as

$$\frac{\mathrm{d}V}{\mathrm{d}t} = -\frac{1}{2}\mu_{\mathrm{eff}}(t)\frac{V_0^2}{d^2} \tag{7}$$

where d is the sample thickness.

2.2. Dispersive mobility

Several authors [24,26–30] have treated dispersive mobility theoretically but, as far as we know, low attention has been paid from the experimental point of view. This behavior has been taken on account by several authors to describe the anomalous transport observed in some photosensitive materials, and it has been extended to different areas successfully, such as fluid dynamics, geology, Brownian motion, as well as to electric transport in insulating materials [30–33].

Scher and Montroll [24] developed a stochastic transport model to explain charge transport in disordered materials. This model is based on the dispersion of the distances between localized sites available for carriers to hop and on the dispersion of the potential barriers between these sites. This distribution in distances and/or energies affects the time a charge needs to hop from one site to another. These charges are supposed to follow a time dependent random walk governed by a waiting-time distribution function $\psi(t)$. The shape of this distribution function will be related to the lack of order of the material. In the reciprocal time domain this function is related to $\eta(t)$ by [24,28]:

$$\mathrm{LT}[\eta(s)] = \frac{s\mathrm{LT}[\psi(s)]}{1 - \mathrm{LT}[\psi(s)]} \tag{8}$$

On the one hand, charge transport in a free of traps ordered material is described by a Gaussian distribution function $\psi(t) \propto \mathrm{e}^{-\beta t}$, where there is no dispersion of the charges' packet and the shape of the charges' distribution is maintained. This corresponds to a constant mobility, $\mu \propto \mu_0\delta(t)$. On the other hand, a dispersive transport regime in a potential decay process is characterized [24] by $\psi(t) \propto t^{-1-\alpha}$, which gives a time dependence of mobility

$$\eta(t) \approx LT^{-1}\left[ks^{1-\alpha}\right] \tag{9}$$

where k is a constant and $0 \le \alpha \le 1$. For the initial stage of the discharge, the time derivative of the surface potential is approximately [28]

$$\frac{dV}{dt} \approx -\frac{k}{2\Gamma(\alpha)}\frac{V_0^2}{d^2}t^{\alpha-1} \tag{10}$$

From this equation $\eta_D(t) = \gamma t^{\alpha-1}$, where γ is a parameter that depends on α, k and the proper mobility μ_0.

This new term, together with the non-dispersive one, results in an effective mobility as

$$\mu_{\text{eff}} = \mu_0\left(\frac{r_r + r_t\ e^{-Rt}}{R} + \gamma t^{\alpha-1}\right) \tag{11}$$

After integration of Eq. (7) with the effective mobility given by Eq. (11) the surface potential of the sample can then be written as

$$V(t) = V_0\left(1 - \frac{\mu_0}{2R}\frac{V_0}{d^2}\left(r_r t + \frac{r_t}{R}\left(1 - e^{-Rt}\right)\right) - \lambda t^{\alpha}\right) \tag{12}$$

where

$$\lambda = \frac{\mu_0 V_0 \gamma}{2d^2\alpha}. \tag{13}$$

3. Experimental

To check the validity of our assumption we have charged several samples of Kapton HN of 50.8 μm thick via the corona triode [34]. The charging device is sketched in Fig. 1.

The samples were metalized on one side. Their non-metalized faces were charged at different initial potentials. The surface potential measurement was carried out with a Trek model 347 electrostatic voltmeter and it began a fraction of a second after the charging process.

The needle of the corona triode was kept at 15 kV during the charging process, with a gap of 25 mm between the grid and the needle. The charging time was 1 s in all cases. The distance between the sample and the grid was 8 mm.

Kapton samples were provided by Dupont and were stored at a temperature between 22 °C and 25 °C and at relative humidity between 40% and 50%. The experiments were carried out in the same environment, in the dark. The influence of elevated humidity on the electrical conductivity of polyimide can be found in the literature [35,36].

4. Results and discussion

In Figs. 2 and 3 we show in lin–log scales the normalized potential versus time for the different charge sign and initial voltages studied. We can appreciate the accuracy of the fit, resulting by taking into account both terms. When the dispersive term was not considered, the slope predicted by the model at the initial step of the charge decay was lower than the one observed experimentally (not shown) so that both mechanisms, dispersive and non-dispersive, are necessary to describe the surface potential decay accurately from the initial stage up to the transit time.

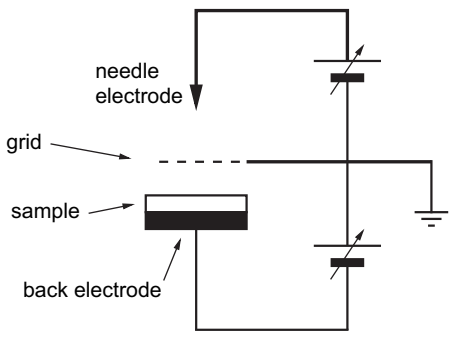

Fig. 1. Sketch of the corona triode charging device.

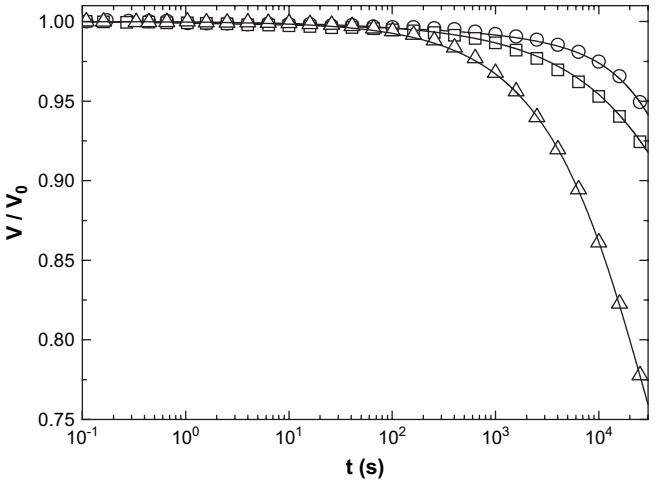

Fig. 2. Normalized surface potential versus time for negative initial potentials. ○: −1000 V, □: −2000 V, △: −3000 V. Lines were calculated after fitting the data to Eq. (12).

The values of free parameters resulting from fitting Eq. (12) to experimental data are shown in Table 1. We can see that the values of the proper mobility of the band depend on neither the initial potential nor the sign significantly, but it seems that the mean value of the mobility for negative carriers is slightly smaller (2.06×10^{-17} m^2 V^{-1} s^{-1}) than for positive carriers (2.37×10^{-17} m^2 V^{-1} s^{-1}).

In Figs. 2 and 3 it can be noticed that the potential decay is faster for higher initial potential. This seems reasonable as a non-field dependent mobility has been assumed and a higher field results in a higher carrier drift velocity. The parameter r_r decreases when the initial field is increased, so it seems more difficult for carriers to escape from traps when a higher initial potential has been applied. As we are considering relatively short times (a time scale smaller than the average time a carrier remains trapped, r_r^{-1}) this decrease indicates that charges get trapped deeper for higher fields. On the other hand r_t seems to decrease for increasing initial surface potential, although this trend is reversed for −3000 V. We related this behavior to a decrease of the potential barriers of the traps associated with the field, which results in a decrease of the trapping rate.

The parameter α can be associated with the sublinear power-law observed in conductivity in the frequency domain [37–40]. This power-law conduction regime is associated with the slowing down of

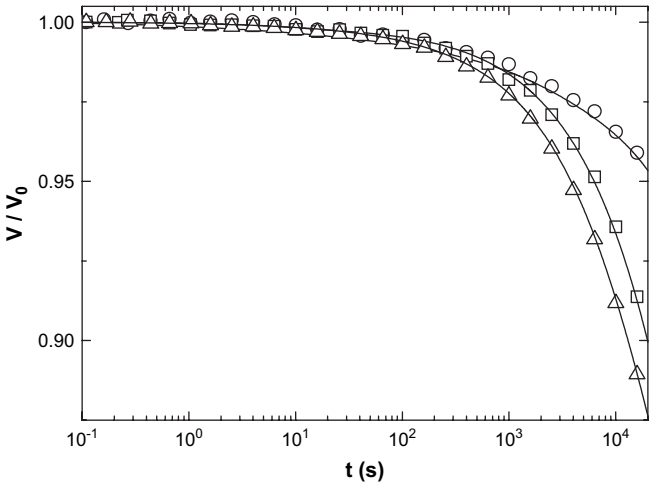

Fig. 3. Normalized surface potential versus time for positive initial potentials. ○: 1000 V, □: 2000 V, △: 3000 V. Lines were calculated after fitting the data to Eq. (12).

Table 1
Parameters of the model calculated by fitting Eq. (12) to experimental data

V_0 (V)	μ_0 ($\times 10^{-17}$ m^2 V^{-1} s^{-1})	r_r (s^{-1})	r_t (s^{-1})	λ (s$^{-\alpha}$)	α
976	2.208	1.61×10^{-4}	8.79×10^{-3}	1.15×10^{-3}	0.367
1814	2.779	1.83×10^{-4}	3.43×10^{-4}	1.21×10^{-3}	0.295
2797	2.126	9.48×10^{-5}	2.10×10^{-4}	1.54×10^{-3}	0.313
−983	2.025	4.63×10^{-4}	6.36×10^{-4}	4.83×10^{-3}	0.094
−2018	2.020	7.01×10^{-5}	2.34×10^{-4}	3.93×10^{-3}	0.129
−3011	2.133	4.13×10^{-5}	5.05×10^{-4}	1.94×10^{-4}	0.687

the relaxation process in the frequency domain as a result of the cooperative effects, in the same way as the KWW function does in the time domain. An important connection between these two approaches stems from the coupling model of Ngai and Kannert [41]. This model predicts a power-law conductivity associated with the KWW relaxation function due to the correlation among charge carriers.

The values of α obtained depend on the sign of the carrier (Table 1). For negative carriers this contribution grows with the initial surface potential, but for positive carriers we do not appreciate a significant dependence on the applied field. We think that this result can be associated with the differences between the trapping level concentrations for holes and electrons. The concentration of traps for holes in this material may be larger than the concentration of traps for electrons, so that the fraction of filled traps for holes is small in all the cases studied and the motion of a given carrier is weakly influenced by neighboring carriers, resulting in a relatively uncorrelated hopping process in all cases. The number of traps for electrons is smaller and we think that between −2 kV and −3 kV the fraction of occupied traps is large enough so that the motion of a given electron is influenced by neighboring trapped carriers, resulting in a more correlated transport process.

5. Conclusions

We have seen that, in order to explain charge decay in Kapton HN polyimide, previous models do not fit well for the first seconds of the decay. They behave quite properly for longer times, but for short times their decay is almost horizontal on lin–log scales, when the experimental plot happens to have a higher slope. It is only taking into account an additional dispersive behavior that the theoretical expression proposed for the potential decay improves the accuracy of the fit. Results also show different behavior for positive and negative charge carriers; while dispersive parameters do not manifest strong changes for positive charges (holes in the conduction band), they do change significantly for negative charges (electrons in the valence band).

Acknowledgments

This research work has been partially supported by Spanish Government Project PTR95.0742.OP.

References

[1] Lai ST. Spacecraft charging threshold in single and double Maxwellian space environments. IEEE Trans Nucl Sci 1991;6:1629–34.
[2] Frederickson AR. Upsets related to spacecraft charging. IEEE Trans Nucl Sci 1996;2:426–41.
[3] Garret HB, Whittlesey AC. Spacecraft charging: an update. IEEE Trans Plasma Phys 2000;6:2017–28.
[4] Frederickson AR, Benson CE, Bockman JF. Measurement of charge storage and leakage in polyimides. Nucl Instrum Methods Phys Res Sect B 2003;208:454–60.
[5] Yin Y, Fang J, Cui Y, Tanaka HKK, Okamoto K. Synthesis, proton conductivity and methanol permeability of a novel sulfonated polyimide from 3-(2′,4′-diaminophenoxy)propane sulfonic acid. Polymer 2003;44:4509–18.
[6] Jiang X, Bin Y, Matsuo M. Electrical and mechanical properties of polyimide–carbon nanotubes composites fabricated by in situ polymerization. Polymer 2005;46:7418–24.
[7] Musto P, Ragosta G, Scarinzi G, Mascia L. Polyimide–silica nanocomposites: spectroscopic, morphological and mechanical investigations. Polymer 2004;45:1697–706.
[8] Baker DN. The occurrence of operational anomalies in spacecraft and their relationship to space weather. IEEE Trans Plasma Sci 2000;28:2007–16.
[9] Quamara JK, Pillai PKC, Sharma BL. Surface potential decay characteristics and TSDC studies in corona charged Kapton polyimide film. Acta Polym 1983;34:265–7.
[10] Coelho R, Levy L, Sarrail D. On the natural decay of corona charged insulating sheets. Phys Status Solidi A 1986;94:289–98.
[11] Centurioni L, Coletti G, Guastavino F. An experimental study to investigate the effects of partial discharges (PD) of electric field and of relative humidity during surface PD tests on thin polymer films. Conference on electrical insulation and dielectric phenomena; 1999. p. 239–42.
[12] Centurioni L, Guastavino F, Tiemblo P, Yang GM, Sessler GM. Charge decay on polymers subjected to ageing by partial discharges. Polym Int 1998;46:47–53.
[13] Chen G, Xiao H, Zhu C. Charge dynamic characteristics in corona-charged polytetrafluoroethylene film electrets. J Zhejiang Univ Sci 2004;8:923–7.
[14] Llovera P, Molinié P. New methodology for surface potential decay measurements: application to study charge injection dynamics on polypropylene films. IEEE Trans Dielectr Electr Insul 2004;11:1049–56.
[15] Chen G, Xu Z, Zhang LW. Measurement of the surface potential decay of corona-charged polymer films using the pulsed electroacustic method. Meas Sci Technol 2007;18:1453–8.
[16] Wintle HJ. Surface-charge decay in insulators with nonconstant mobility and deep trapping. J Appl Phys 1972;43:2927–30.
[17] Sonnonstine TJ, Perlman MM. Surface-potential decay in insulators with field-dependent mobility and injection efficiency. J Appl Phys 1975;46:3975–81.
[18] Toomer R, Lewis TJ. Charge trapping in corona-charged polyethylene films. J Phys D Appl Phys 1980;13:1343–56.
[19] Campos M, Giacometti JA. Surface-potential decay in insulators with deep traps. J Appl Phys 1981;52:4546–52.
[20] von Berlepsh H. Interpretations of surface potential kinetics in HDPE by a trapping model. J Phys D Appl Phys 1985;18:1155–70.
[21] Mott NF, Davis EA, editors. Electronic processes in non-crystalline materials. Oxford: Oxford University Press; 1971.
[22] Seanor DA, editor. Electrical properties of polymers. London: Academic Press; 1982.
[23] Sessler GM, editor. Electrets, vol. 1. California, USA: Laplacian Press; 1998.
[24] Scher H, Montroll EW. Anomalous transit-time dispersion in amorphous solids. Phys Rev B 1975;12:2455–77.
[25] Sidebottom DL, Green PF, Brow RK. Anomalous-diffusion model of ionic transport in oxide glasses. Phys Rev B 1995;51:2770–6.
[26] Mady F, Renoud R, Ganachaud J-P, Bigarré J. Potential decay experiments for the characterization of electron transport. Modelling and discussion. Phys Status Solidi B 2005;242:2089–106.
[27] Shlesinger MF. Asymptotic solutions of continuous-time random walks. J Stat Phys 1974;10:421–34.
[28] Ferreira GFL, Carrano LE. Space-charge transport in disordered media. Phys Rev B 1997;56:11579–83.
[29] Kehr KW, Murthy KPN, Ambaye H. Connection between dispersive transport and statistics of extreme events. Physics A 1998;253:9–22.
[30] Picos-Vega A, Ramírez-Bon R. Transient transport in disordered multilayers. Phys Rev B 2001;64: 014201-1–014201-5.
[31] Berkowitz B, Scher H. Anomalous transport in random fracture networks. Phys Rev Lett 1997;79:4038–41.
[32] Shlesinger MF, Klafter J, Zumofen G. Above, below and beyond Brownian motion. Am J Phys 1999;67:1253–9.
[33] Berkowitz B, Scher H, Silliman SE. Anomalous transport in laboratory-scale, heterogeneous porous media. Water Resour Res 2000;36:149–58.
[34] Dias CJ, Marat-Mendes JN, Giacometti JA. Effects of a corona discharge on the charge stability of Teflon FEP negative electrets. J Phys D Appl Phys 1989;22:663–9.
[35] Belluci F, Khamis I, Senturia SD, Latanision RM. Moisture effects on the electrical conductivity of Kapton polyimide. J Electrochem Soc 1990;137:1778–84.
[36] Galichin NA, Borisova ME. The influence of elevated humidity on the stability of the electret state in polyimide films. Russ Electr Eng 2007;78:129–32.
[37] Shlesinger MF, Montroll EW. On the Williams–Watts function of dielectric relaxation. Proc Natl Acad Sci USA 1984;81:1280–3.
[38] Milovanov AV, Rypdal K. Stretched exponential relaxation and AC universality in disordered dielectrics. Phys Rev B 2007;76:104201-1–104201-8.
[39] Mudarra M, Belana J, Cañadas JC, Diego JA, Sellarès J. Space charge relaxation in polyetherimides by electric modulus formalism. J Appl Phys 2000;88:4807–12.
[40] Mudarra M, Díaz-Calleja R, Belana J, Cañadas JC, Diego JA, Sellarès J, et al. Sublinear dispersive conductivity in poly(methyl methacrylate) at temperatures above the glass transition. Polymer 2004;45:2737–42.
[41] Sidebottom DL, Green PF, Brow RK. Two contributions to the AC conductivity of alkali oxide glasses. Phys Rev Lett 1995;74:5068–71.